Some Results of Powered Glider Flights During PUKK

By Jörg M. Hacker, Meteorologisches Institut der Universität Bonn, W. Germany

Paper presented at the XVIII. OSTIV Congress, Hobbs, New Mexico, USA

Abstract:

During the field experiment PUKK at the coast of the German Bight three instrumented powered gliders were used to investigate the planetary boundary layer over sea and land. First evaluations of the aircraft data give a comprehensive picture of the influence of the coast on the turbulence, temperature and humidity pattern. For selected cases the horizontal wind vector could be determined and showed good agreement with independent measurements. The temporal and spatial variations of the vertical energy fluxes are presented for the coastal region and an area over the flat countryside 80 km inland. For the inland area the mean horizontal wind divergence could be estimated.

Introduction:

In the fall of 1981 the field experiment PUKK (Projekt zur Untersuchung des Küstenklimas) took place at the coast of the German Bight. Among the purposes of the experiment was the investigation of the structure of the planetary boundary layer (PBL) over sea and land and the associated energy fluxes.

While the lowest 10 to 100 m of the atmosphere could be sounded by ground-based or tower-mounted instrumentation, the higher levels required balloon- or aircraft-mounted systems. Balloon-borne probes gave a reasonable picture of the vertical structure at different locations of the experimental area; aircraft, including a fleet of three powered gliders, were used to achieve a detailed picture of the horizontal and vertical structure of the boundary layer. In the following, first results of the flights with the powered gliders, including a few comparisons with independent measurements, will be given.

Instrumentation and Data Processing

The powered gliders are operated by the DFVLR (Deutsche Forschungs- und Versuchsanstalt für Luft- und Raumfahrt), the instrumentation has been developed by the DFVLR's Institute of Atmospheric Physics and is identical for all three aircraft. Several meteorological and aircraft parameters are measured and recorded digitally on magnetic tape.

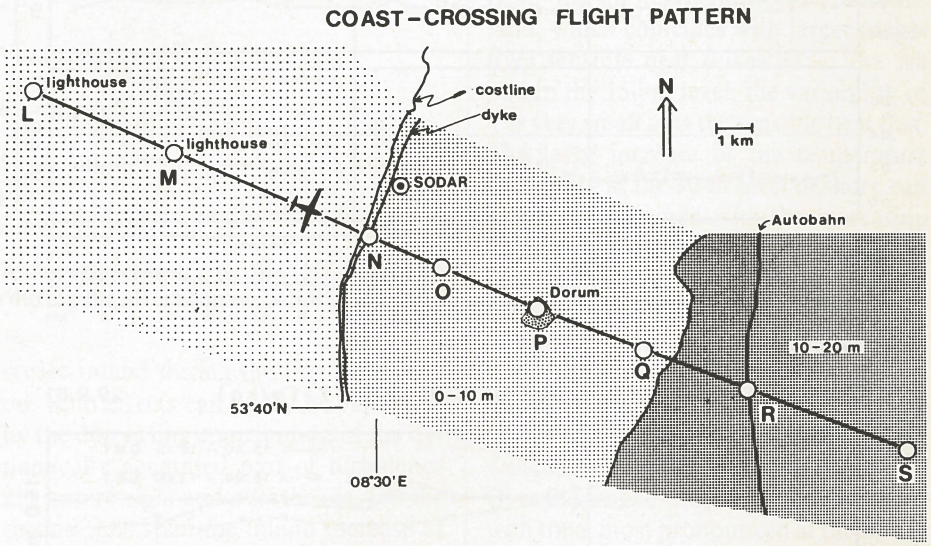

Fig. 1 Sketch of the coast-crossing flight pattern. Bold straight line segments: flight path; L to S: ground reference points; ⊙ approximate location of the Doppler-Sodar array of the Max-Planck-Institut für Meteorologie; light shading: sea and tidal flats; medium shading: land lower than 10 m MSL; dark shading: land between 10 m and 20 m MSL.

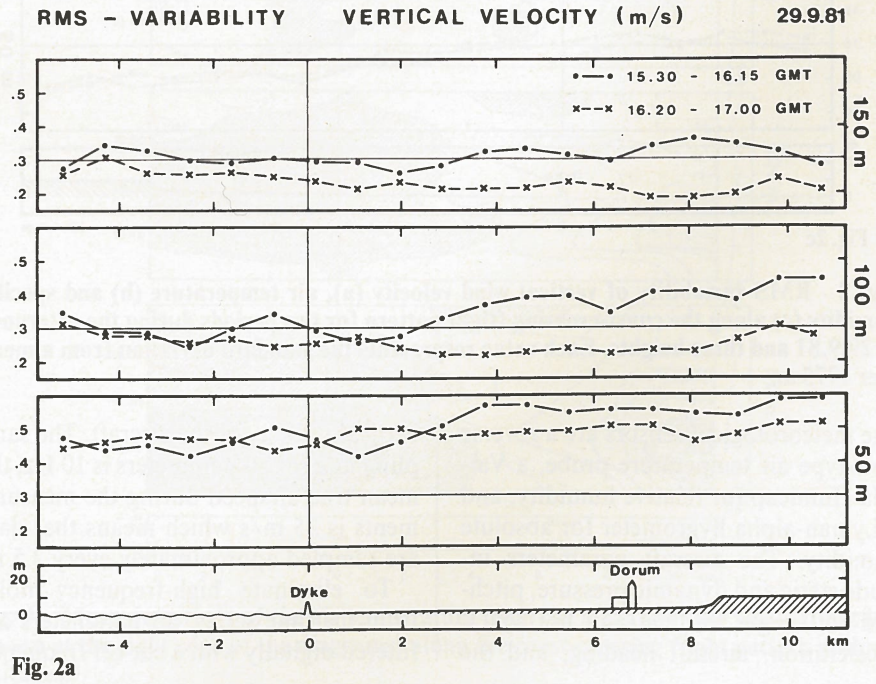

Fig. 2a

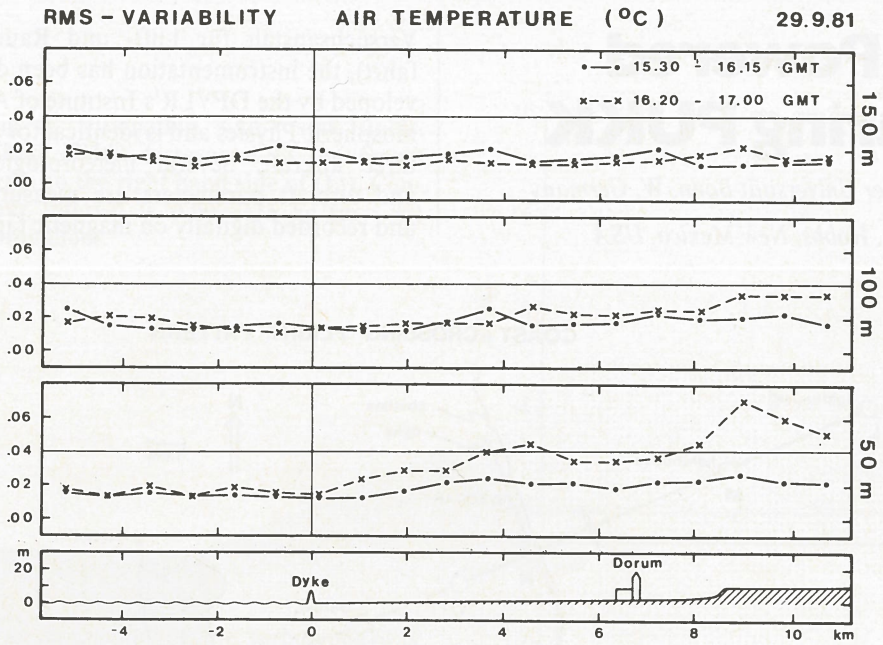

Fig. 2b

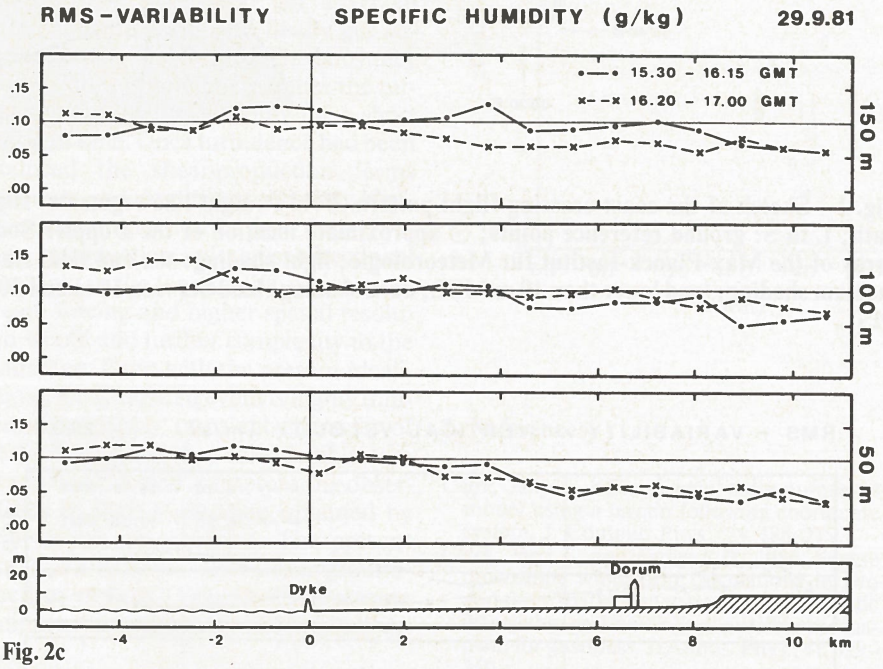

Fig. 2c

Fig. 2 RMS variability of vertical wind velocity (a), air temperature (b) and specific humidity (c) along the coast-crossing flight pattern for two periods during the afternoon of 29.9.81 and three heights. Each value respresents the standard deviation from a mean over 1775 m.

The meteorological sensors are a reverse flow-type air temperature probe, a Vaisala Humicap for relative humidity, and a Lyman-alpha hygrometer for absolute humidity. The aircraft parameters include static and dynamic pressure, pitch- and roll angle, vertical and horizontal acceleration, aircraft heading, and the vertical velocity of the aircraft. The sampling rate for all parameters is 10 Hz, the mean true airspeed during the measurements is 35 m/s which means that data are sampled approximately every 3.5 m.

To eliminate high-frequency noise from the time series, all parameters are filtered digitally with a cut-off frequency of 2 Hz (corresponding to approximately 17.5 m). For the computation of the vertical energy fluxes, the final time series of vertical air velocity, specific humidity and air temperature were high-pass filtered with a cut-off frequency of 0.01 Hz which eliminates contributions to the fluxes with length scales longer than about 3.5 km. This upper boundary for the considered length scale was chosen, because the length of the flight legs as well as the response characteristics of the aircraft to atmospheric motions prohibited proper resolution of larger-scale fluxes.

The temperature measurements were corrected for height variations by reducing each temperature value to a reference pressure level using a vertical temperature gradient derived from the respective flight leg. The humidity measurements of the Vaisala Humicap sensor and the Lyman-alpha sensor were combined, using the Humicap for the slow and the Lyman-alpha for the fast humidity variations, with a cross-over frequency of 0.2 Hz. The vertical velocity of the air w_a cannot be measured directly with the current instrumentation of the powered gliders. Therefore the aerodynamic lift equation was used to compute w_a from other aircraft parameters. A description of the computational scheme is given in Hacker (1982). To obtain an estimate of the mean horizontal wind from the aircraft measurements, a method was used, which requires no information about the aircraft heading. Since with the present instrumentation the measurement of the heading involves several possible errors, this method showed much more reliable results than the normal one using ordinary wind triangles. The procedure is descibed in Hacker (1982).

Presentation of the Results

During the experiment two different strategies were used to investigate the PBL with the powered gliders in connection with ground stations. The first pattern was designed to get a comprehensive picture of the small- and mesoscale effects (about 10 m to 10 km) which are generated by the change of roughness and thermal properties in the vicinity of the coastline. The second pattern was

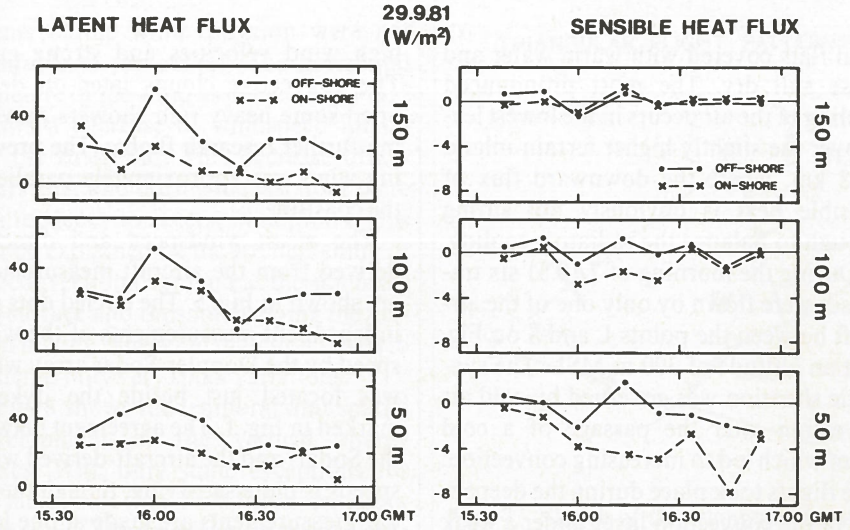

Fig. 3 Vertical fluxes of latent (left) and sensible (right) heat over sea (offshore) and land (onshore) at three altitudes for the flights during the afternoon of 29.9.81.

laid out to give an estimate of the energy budget of a limited area in the flat countryside about 80 km inland and the possibility of comparing vertical energy fluxes and wind measured from tethered balloons and powered gliders. The results of the coastal pattern will be presented first.

The Influence of the Coastline on the Boundary Layer

On 29.9.81 flights were made approximately perpendicular to the coastline according to Fig. 1. The three aircraft flew eight traverses at 50 m, 100 m and 150 m MSL between the points M and R simultaneously. The flights took place between 15.30 and 17.00 GMT, covering the 1.5 hours before sunset. The prevailing wind direction was about 270 to 280 degrees at the ground, not substantially changing with height. The weather conditions were governed by a weak high-pressure cell which led during the day to shallow convection under a subsidence inversion at about 1000 m. During the flights the convection weakened to less than ⅛ Cu hum with bases at about 500 m.

The spatial variations of the rms variability of vertical wind velocity w_a, air temperatur T and specific humidity q are shown in Fig. 2 for two time periods. The two most obvious features of Fig. 2a are the pronounced decrease of the variability of w_a with height, and the slight increase inland during the first time period. Both effects can partly be explained by the decreasing contribution of the dynamically generated part of turbulence at greater height and over the sea. For the second time span the inland increase of the turbulence seems to vanish, perhaps again caused by reduced dynamic turbulence due to the decrease of the windspeed from 7.2 m/s at 15.00 GMT to 4.7 m/s at 17.00 GMT.

The buoyancy-generated contribution to the turbulence pattern can be inspected with the help of the Figs. 2b and 2c and the energy fluxes shown in Fig. 3. Except for the 150-m level, the variability of the air temperature increases inland, which coincides with larger (negative) sensible heat fluxes. Over the sea and in the 150-m level, the variability of T is very small as is the sensible heat flux. The large increase of the temperature variability at the 50-m level onshore can easily be explained with the increasing downward flux of sensible heat to overcome the radiative cooling of the land surface.

With respect to spatial variations, the variability of the specific humidity shows a pattern somewhat reverse to that of the temperature. The reason is the weakening of the convection over land. Over the sea the variability of q increases with time, most pronounced at the 100-m level, and this is explained by the rising

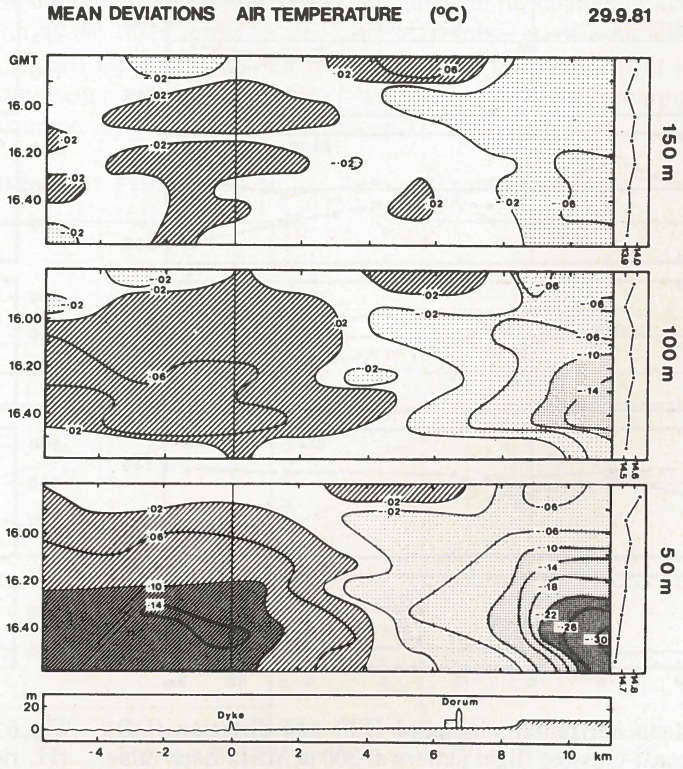

Fig. 4 Mean deviations of the air temperature from the mean over the whole flight leg (shown at the right edge of the diagrams) along the coast-crossing flight pattern at three altitudes.

tide which increasingly covers the offshore tidal flats with relatively warm water. A similar consequence of the rising tide is the offshore increase of the latent heat flux between 16.20 and 17.00 GMT.

Fig. 4 gives a detailed picture of the development of air temperature in time and space. Depicted are the mean deviations from the mean temperature over each respective traverse. The mean temperature for each traverse is given at the right edge of Fig. 4. It can be seen that the influence of the warm tidal waters reaches inland to about the township of Dorum. The area of large positive deviations between 0 and -2 km offshore may be due to slightly increased convection generated by the sharp small-scale thermal contrasts between those areas of the tidal flats covered with warm water and those still dry. The most pronounced cooling of the air occurs in the lowest level over the slightly higher terrain inland of 8 km, where the downward flux of sensible heat is obviously not strong enough to balance the radiative cooling.

During the morning of 7.10.81 six traverses were flown by only one of the aircraft between the points L and S on Fig. 1 at an altitude of 300 m MSL. The synoptic situation was governed by cold air advection after the passage of a cold front which led to increasing convection. The flights took place during the deepening of the convection layer under a weak subsidence inversion at about 1000 m. The flight conditions in this convection layer were rather difficult because of the high wind velocities and strong gusts. The convective clouds later on developed some heavy rain showers preventing further research flights. The prevailing wind was approximately parallel to the coastline.

The mean windspeed and direction derived from the aircraft measurements are shown in Fig. 5. The circled dots give independent measurements of the windspeed by the Doppler-Sodar array which was located just beside the dyke as marked in Fig. 1. The agreement between the Sodar- and the aircraft-derived windspeeds is quite satisfying, though the Sodar measurements are made at one location, while the aircraft winds are means over the area covered by the flightpath. Unfortunately, independent measure-

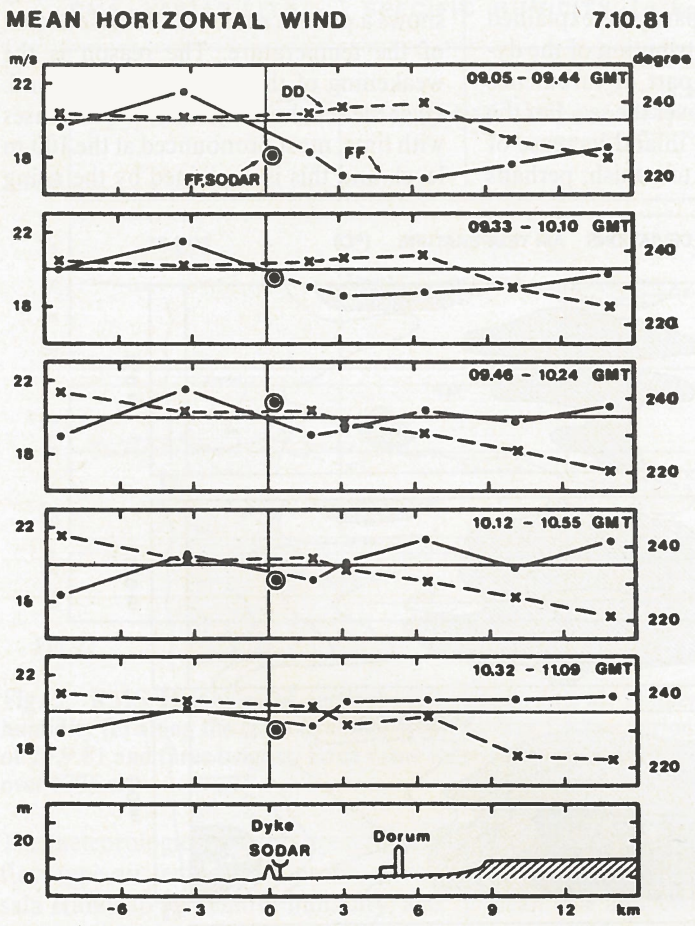

Fig. 5 Mean horizontal windspeed (FF) and direction (DD) along the coast-crossing flight pattern at 300 m MSL. Each value represents the mean for the flight between two adjacent visual fixes (see Figure 1) and two successive flight legs. The encircled dots give mean windspeeds derived from Doppler-Sodar measurements of the Max-Planck-Institut für Meteorologie at the location shown in Figure 1.

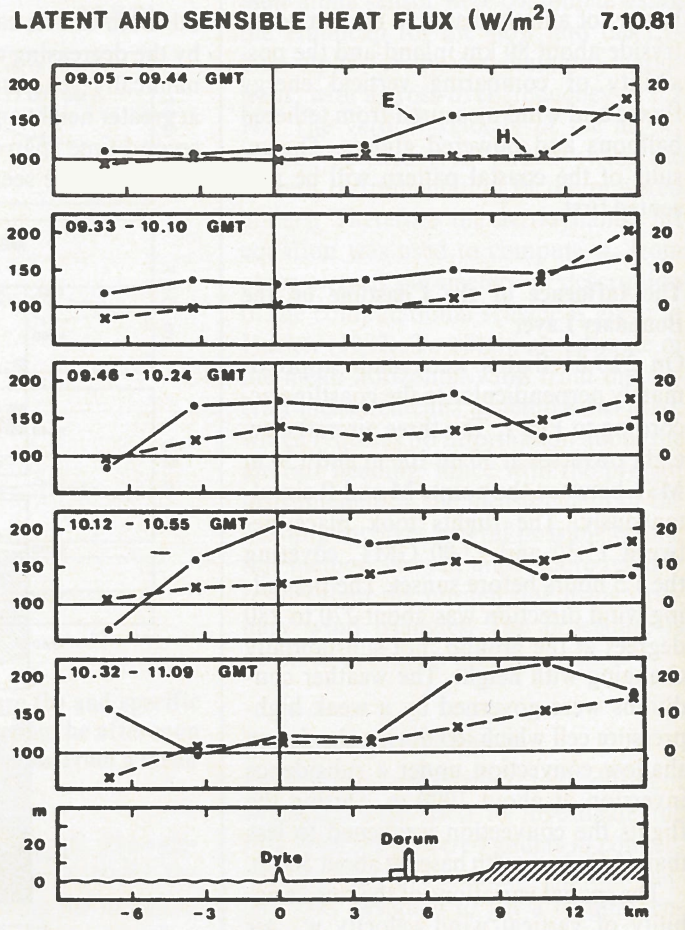

Fig. 6 Mean vertical fluxes of latent (E, left scale) and sensible (H, right scale) heat along the coast-crossing flight pattern at 300 m MSL. Each value represents the mean over two successive flight legs and 7050 m.

ments of the wind direction were not available to the author. The horizontal structure of the wind as depicted in Fig. 5 shows a decrease of windspeed inland for the first hour. This decrease disappears later and during the last hour there is a tendency to reverse conditions. This can be explained by the strengthening of the convection over land as the sun heats the surface and thus intensifying the vertical mixing. The wind direction seems to undergo only very small variations.

Fig. 6 shows the temporal and spatial development of the vertical energy fluxes. With only some exceptions for the latent heat flux, both fluxes are larger over land. The build-up of the sensible heat flux with increasing warming of the underlying surface can clearly be seen, as well as the influence of the change from moist marshy to drier sandy soils about 9 km on-shore, especially for the two first time periods. The latent heat flux shows a large variability which is presumably connected with larger convection cells. It seems in fact that the size of the convection cells was sometimes larger than 3 to 4 km, the largest length scale which can be properly measured with these aircraft.

The Structure of the PBL over a Flat Area

80 km inland from the coast a triangular array of three tethered balloons and an energy balance station had been established to investigate the vertical energy fluxes and the energy budget over this flat area. To compare these independently measured energy fluxes with fluxes derived from the aircraft data, several flights were made over this area. A sketch of the flight pattern is given in Fig. 7.

On 30.9.81 flights with all three aircraft were made around the triangle during the development of shallow convection under a subsidence inversion which rose from about 500 m to about 1000 m. The synoptic situation was dominated by a weak high-pressure cell in the northeast of the experimental area, producing slight south to southwesterly winds. The aircraft flew at 150 m, 300 m and 450 m above the ground simultaneously along the sides of the triangle. Between 10.50 and 12.50 GMT the triangle was circumnavigated three times, thus giving

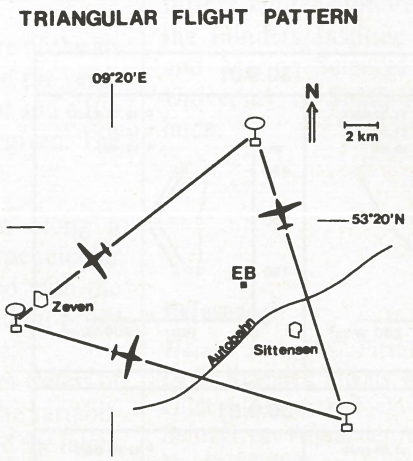

Fig. 7 Sketch of the triangular array 80 km inland from the coast. The three tethered balloons were placed at the corners of the triangle and the energy balance station (EB) inside the area. The flights were made along the sides of the triangle counterclockwise.

nine flight legs per aircraft. In the following, only the results of the aircraft measurements will be presented, because other datasets were not yet available to the author.

Fig. 8 shows the changes of windspeed and direction at the three levels as derived from aircraft measurements. Each datapoint represents a mean value for the whole triangle. The vertical consistency of the changes in the time series is remarkable, particulary considering the smallness of the changes. Encouraged by these results, a determination of the mean wind divergence over the triangle was attempted. The computed divergences are 1.84×10^{-5} s^{-1} at 150 m,

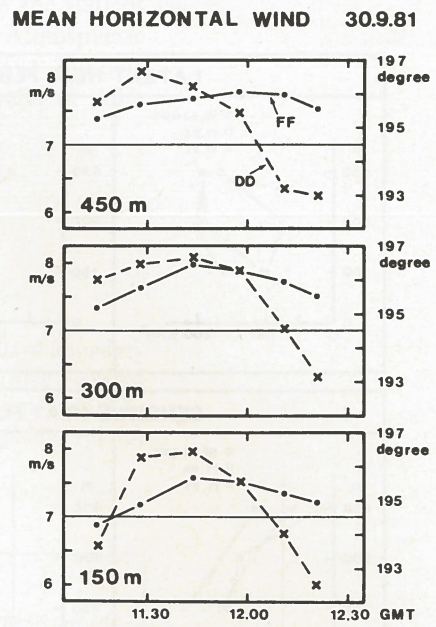

Fig. 8 Mean horizontal windspeed (FF) and direction (DD) for the triangle at three altitudes. Each value represents an average over the whole triangle.

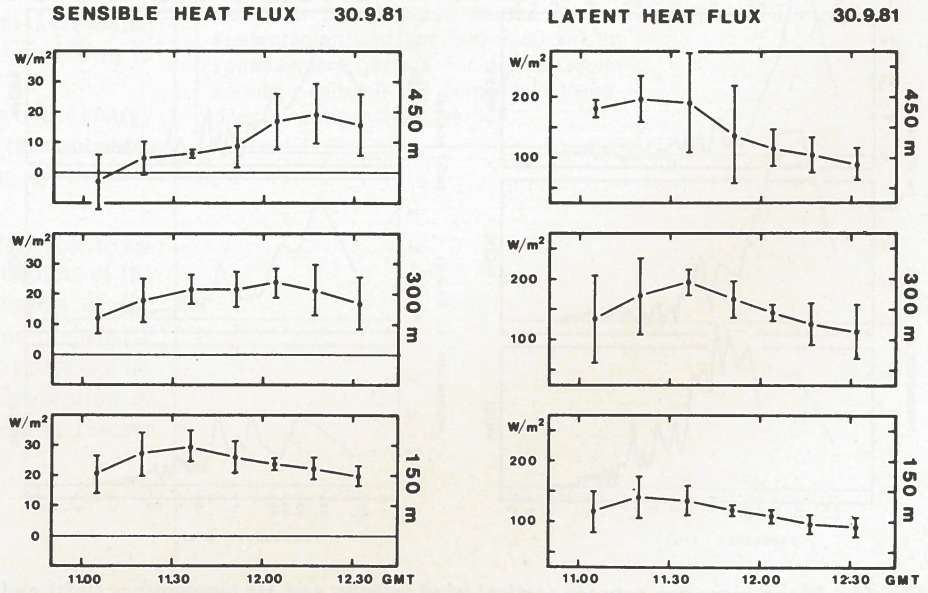

Fig. 9 Mean vertical fluxes of sensible (left) and latent (right) heat for the triangle at three altitudes. Each value represents an average over a complete flight around the triangle, that means three flight legs. The variability bars show the standard deviation from these averages.

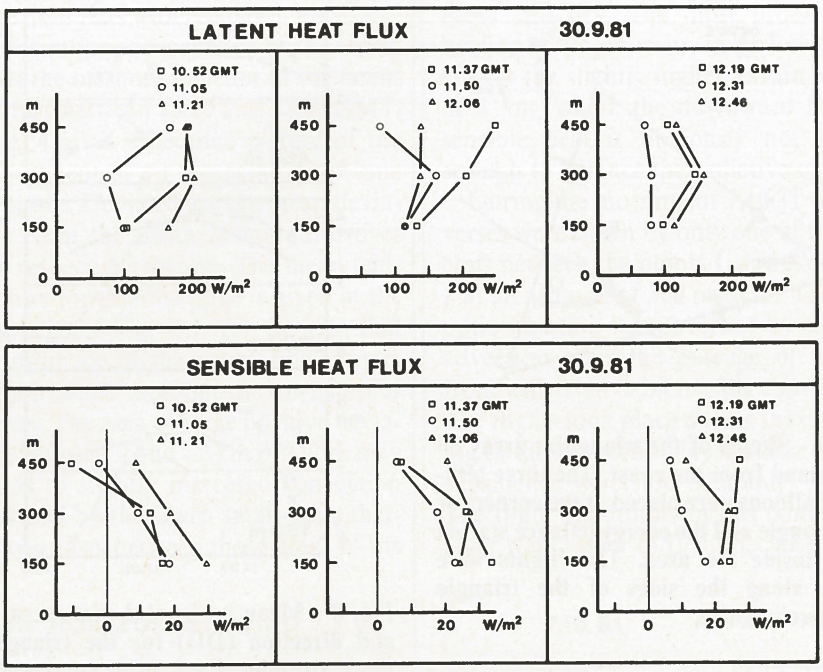

Fig. 10 Profiles of the vertical flux of latent (top) and sensible (bottom) heat for the flight legs around the triangle. The first profile refers to the northeastern side of the triangle, the second to the northwestern side, etc.

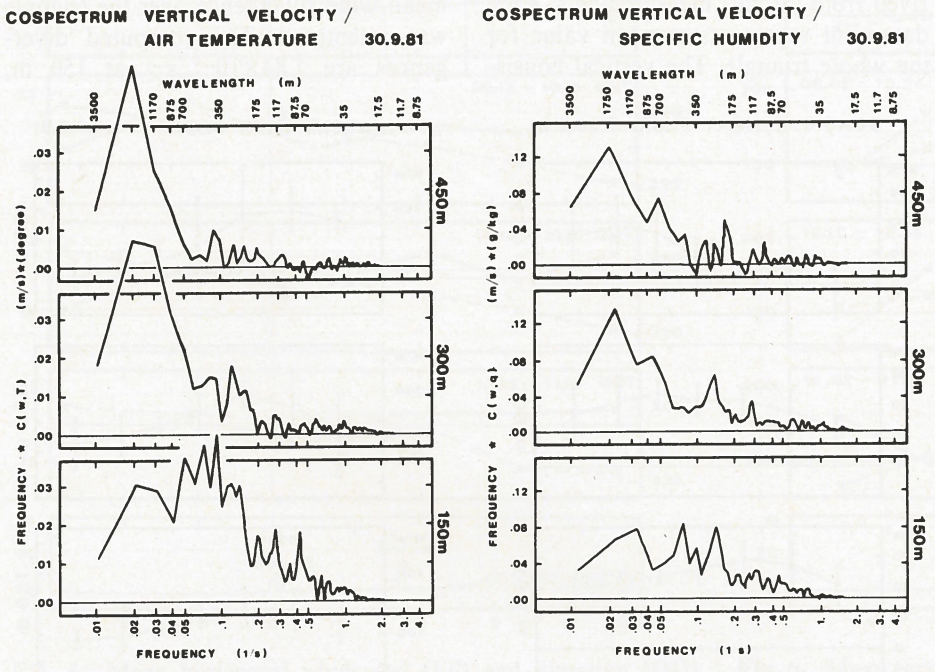

Fig. 11 Mean cospectra between vertical wind velocity and air temperature (left) and vertical wind velocity and specific humidity (right) for the second flight around the triangle, consisting of the flight legs in the second diagrams of Figure 10 (top and bottom). The wavelengths at the top of the diagrams were computed with a mean true airspeed of 35 m/s. All spectra were smoothed over 10% of the actual wavelength.

$1.31 \times 10^{-5}\ s^{-1}$ at 300 m and $1.13 \times 10^{-5}\ s^{-1}$ at 450 m. These divergences are not unlikely under the given synoptic situation. Again the consistency between the tree levels is surprisingly good.

The fluxes of sensible heat H and latent heat E of Fig. 9 are running means of successive flight legs around the whole triangle to eliminate the influence of the wind direction. The variability bars give the rms variability between the three sides of the triangle. The variability of the fluxes is found to be very high, about 50 to 100% of the individual flux. Nevertheless, the consistency of the development of the fluxes between the three levels supports their reliability.

The vertical structure of H and E is shown in greater detail in Fig. 10. Each profile of H and E is now computed as mean over one side of the triangle, starting at 10.52 GMT at the southeastern corner and proceeding counterclockwise around it. As mentioned earlier, the convective layer was topped by an inversion which could be found at approximately 500 m during the first flight legs. Later the inversion rose to about 1000 m. This is in good agreement with the vertical structure of the sensible heat flux. During the first hour, H decreases strongly with height, tending to negative values just below the inversion. Later H becomes nearly constant with height, but a slight tendency to a decrease with height still remains. Furthermore, the increase of E as well as the decrease of H with height during the first hour may be connected with the advection of relative cold and moist air, but a definitive interpretation is not possible with the datasets currently available.

The horizontal scales which contribute to the fluxes can be seen on the plots of the cospectral densities for w_a and T and for w_a and q, respectively, in Fig. 11. The cospectra show that the largest contributions shift to larger wavelengths with height, as would be expected. While for the 150-m level the main contributions come from scales between 150 m and 500 m, the main contributions at the 450-m level seem to come from scales larger than 1000 m. From this it could be suspected that a certain kind of meso-scale organisation was superimposed over the convection pattern.

Conclusions:

Some examples of the structure of the atmospheric boundary layer and the vertical energy fluxes over the coast and a flat area 80 km inland have been given. The prominent features are:

a) The turbulence pattern along a flightpath approximately perpendicular to the coast can be connected with the changes in roughness and thermal properties of the underlying surface.

b) The influence of the warm waters of the rising tide can be seen in the variability of the specific humidity and the latent heat flux. The influence of these tidal waters seems to reach approximately 5 km onshore in this case.

c) The effects of the radiative cooling of the land surfaces at the evening on air temperature in different levels and the strengthening of the downward sensible heat fluxes over these areas can be estimated.

d) A comparison of the aircraft winds with independent measurements shows satisfying results.

e) The vertical energy fluxes and the horizontal wind vectors for the area 80 km inland show good consistency for the three investigated altitudes, though the variability of the fluxes is 50 to 100% of the individual values.

f) The mean divergence of the horizontal wind over the inland area is estimated to vary from 1.3×10^{-5} s^{-1} in 150 m to 2.7×10^{-5} s^{-1} in 450 m.

g) Spectral investigations of the energy fluxes show the increase of the contributing wavelengths with height.

Finally, it is obviously desirable to relate these and further evaluations of the aircraft data to other datasets of the experiment to get a more comprehensive picture of the atmospheric processes involved. A more detailed description of the presented results is given in Hacker (1982).

Acknowledgements

I wish to thank the staff of the Institute for Atmospheric Physics of the DFVLR for their excellent cooperation in all phases of the experiment. My work was further kindly supported by the staff of the Flinders Institute for Atmospheric and Marine Sciences at The Flinders University of South Australia at Adelaide.

Reference:

Hacker, J.M., 1982: First Results of Boundary Layer Research Flights With Three Powered Gliders During the Field Experiment PUKK. Beiträge zur Physik der Atmosphäre, Vol. 55, No. 4, 383–402.

Zusammenfassung

Jörg M. Hacker: Erste Ergebnisse der Motorseglerflüge in der Grenzschicht während des Experiments PUKK

Während des Experiments PUKK, das an der deutschen Nordseeküste stattfand, wurde die atmosphärische Grenzschicht über Land und See mit Hilfe von drei instrumentierten Motorseglern untersucht. Erste Ergebnisse dieser Flugzeugmessungen zeigen ein deutliches Bild des Einflusses der Küste auf die Struktur der Turbulenz-, Temperatur- und Feuchtefelder. Für einige Fälle konnte der horizontale Windvektor bestimmt und mit unabhängigen Messungen verglichen werden; es zeigte sich eine gute Übereinstimmung. Die zeitlichen und räumlichen Variationen der vertikalen Energieflüsse werden für die Küstenregion und ein Gebiet 80 km im Landesinnern gezeigt. Für dieses Gebiet konnte zusätzlich die horizontale Winddivergenz abgeschätzt werden.